Eur Biophys J (1995) 23: 423–432

European Biophysics Journal

A long lifetime component in the tryptophan fluorescence of some proteins

Klaus Döring, Lars Konermann *, Thomas Surrey, Fritz Jähnig

Max-Planck-Institut für Biologie, Abteilung Membranbiochemie, Corrensstrasse 38, D-72076 Tübingen, Germany

Received: 9 May 1994 / Accepted in revised form: 24 November 1994

Abstract. The tryptophan fluorescence of two membrane proteins (outer membrane protein A and lactose permease), a 21-residue hydrophobic peptide, three soluble proteins (rat serum albumin, ribonuclease T_1, and azurin), and N-acetyltryptophanamide (NATA) was investigated by time-resolved measurements extended over 65 ns. A long lifetime component with a characteristic time of 25 ns and an amplitude below 1% was found for outer membrane protein A, lactose permease, the peptide in lipid membranes, and azurin in water, but not for rat serum albumin, ribonuclease T_1, and NATA in water. When outer membrane protein A was dissolved and unfolded in guanidinum hydrochloride, the long lifetime component disappeared. Hence, a hydrophobic environment seems to be a necessary requirement for the long lifetime component to be present. However, NATA dissolved in butanol does not exhibit the long lifetime component, while the peptide dissolved in the same solvent under conditions which preserve its helical structure does show the long lifetime. Thus, a regular secondary structure for the polypetide chain to which the tryptophan residue belongs seems to be a second necessary requirement for the long lifetime component to be present. The long lifetime component may therefore be seen in the context of protein substates.

Key words: Time-resolved fluorescence – Multi-exponential decay – Protein substates – Unfolded protein – NATA

* *Present address:* Max-Planck-Institut für Strahlenchemie, Stiftstrasse 34–36, D-45470 Mülheim an der Ruhr, Germany

Abbreviations: OmpA, outer membrane protein A; LP, lactose permease; RSA, rat serum albumin, RNAse T_1, ribonuclease T_1; P21, 21-residue peptide; NATA, N-acetyltryptophanamide; PTP, paraterphenyl; POPE, palmitoyloleoylphosphatidylethanolamine; POPC, palmitoyloleoylphosphatidylcholine; POPG, palmitoyloleoylphosphatidylglycerol; GdHCl, guanidinium hydrochloride

Correspondence to: F. Jähnig

Introduction

The amino acid tryptophan is of special interest in the study of proteins, because it is an intrinsic fluorophore, and its intensity is the strongest of all intrinsic fluorophores. Numerous studies have been performed to characterize the tryptophan fluorescence of proteins and the most detailed data come from single tryptophan proteins (for a review see Beecham and Brand 1985). The excitation and emission spectra of the tryptophan fluorescence appear to involve two states, usually labeled ^1L_a and ^1L_b. The ^1L_a state has the larger transition moment and irradiation at 300 nm leads almost exclusively to excitation of that state, while the ^1L_b state is excited predominantly at 280 nm. When the ^1L_a state is excited at 300 nm, the fluorescence light is emitted in the range 330–360 nm. Hence, for these excitation and emission wavelengths one lifetime of the tryptophan fluorescence is expected and this is indeed found in some cases, the most notable one being N-acetyltryptophanamide (NATA) with a lifetime of about 3 ns (Szabo and Rayner 1980; Wijnaendts van Resandt et al. 1980; Robbins et al. 1980; Ross et al. 1981; Chang et al. 1983; Petrich et al. 1983; Wagner et al. 1987; Bismuto et al. 1991; Vekshin et al. 1992). However, the amino acid tryptophan already exhibits two lifetimes (at neutral pH). Comparative studies on dipeptides led to the proposal that the occurrence of different lifetimes is related to the existence of different rotamers about the C_α–C_β bond (Petrich et al. 1983; Wagner et al. 1987).

The concept of different conformational states and, therefore, different lifetimes is especially useful for tryptophan residues in proteins. Up to 4 lifetimes have been reported with typical values of 0.5, 3, 6, and 10 ns (for recent reports see Gallay et al. 1993; Godik et al. 1993). This heterogeneity has been interpreted in terms of conformational substates in proteins (Ansari et al. 1985). The heterogeneity has even been extended to cover a distribution of lifetimes around each mean lifetime (Alcala et al. 1987 a). Another interpretation has been given by neglecting different substates and instead invoking different mechanisms of energy transfer in one state (Bajzer and

Prendergast 1993). The concept of substates, however, gains more and more support, both from experiment and from computer simulations. Different substates may actually exist and different mechanisms of energy transfer and quenching in some of them may give rise to different lifetimes.

The detection of substates with different lifetimes by fluorescence depends on two requirements: (i) the fluorescence must be sensitive to differences in the conformation of the substates, and (ii) the fluorescence lifetime must be shorter than the lifetimes of the substates (Alcala et al. 1987b). When the fluorescence lifetime is much longer than the lifetimes of the substates, the fluorescence signal is an average over the set of substates and a mean fluorescence lifetime is observed. Hence, the observation of a long fluorescence lifetime indicates the existence of a long-lived substate.

As mentioned already, the tryptophan fluorescence of proteins seems to be sensitive to protein conformation and lifetimes up to 10 ns have been detected, indicating the existence of substates with lifetime of at least 10 ns. However, substates with longer lifetimes are thought to exist in proteins. This raises the question of whether or not it is possible to detect longer lifetimes and thus demonstrate the existence of longer-lived substates. In this paper, we report on the detection of a long lifetime component in the tryptophan fluorescence of some proteins. The lifetime is about 25 ns and the proteins studied are two membrane proteins (outer membrane protein A (OmpA) and lactose permease (LP) of *Escherichia coli*), a hydrophobic peptide of 21 residues (P21), and three soluble proteins (rat serum albumin (RSA), ribonuclease T_1 (RNAse T_1), and azurin). For comparison, NATA was included in the study.

Materials and methods

Materials

RSA, Azurin, NATA, and para-terphenyl (PTP) were obtained from Sigma (München, Germany), phenanthrene was from Serva (München, Germany), all other chemicals were from Merck (Darmstadt, Germany). The lipids palmitoyloleoylphosphatidylethanolamine (POPE), palmitoyloleoylphosphatidylcholine (POPC), and palmitoyloleoylphosphatidylglycerol (POPG) were purchased from Avanti (Alabaster, AL).

P21 was a gift from W. Beck and G. Jung (University of Tübingen, Germany) and was synthesized as described previously (Voges et al. 1987). Its sequence is H-(Ala-Aib-Ala-Aib-Ala)$_3$-Trp-(Ala-Aib-Ala-Aib-Ala)-O-Me with Aib denoting aminoisobutyric acid. RNAse T_1 was a gift from S. Walter and F.X. Schmid (University of Bayreuth, Germany).

Sample preparation

The samples of OmpA were prepared from a stock solution of OmpA (1 mM) which was obtained as described previously (Surrey and Jähnig 1992). OmpA in guanidinium hydrochloride (GdHCl) was prepared by diluting the stock solution into 6 M GdHCl, 20 mM potassium phosphate, pH 7.3, to a final concentration of 5 μM OmpA.

The sample of OmpA in lipid was prepared by a procedure which represents a slight modification of the one described previously (Surrey and Jähnig 1992) and increases the percentage of OmpA being refolded to 95%. In brief, refolding in micelles of the detergent octylglucoside at pH 10 was followed by conventional reconstitution into vesicles of a mixture of 80% POPC and 20% POPG. Final concentrations were 10 mM potassium phosphate, pH 7.4, 100 mM NaCl, and 5 μM OmpA at a lipid/protein mole ratio of 500. Subsequent extrusion through nuclepore filters resulted in vesicles with a mean diameter of 80 nm. The vesicle radius was determined by quasi-elastic light scattering (Coulter N4/SD).

The sample of LP in lipid was prepared as described previously (Dornmair and Jähnig 1989), except that the lipid used for reconstitution was a mixture of 80% POPE and 20% POPG, and the buffer was the same as above. After extrusion through nuclepore filters, the mean vesicle size was determined as 100 nm. The final concentration of LP was 1 μM, and the lipid/protein mole ratio was 1000.

The sample of P21 in butanol was prepared from a stock solution of P21 in methanol (100 mM) and dilution to a final concentration of 30 μM in water-saturated butanol. The sample of P21 in lipid was prepared from the same stock solution of P21 and the above mixture of 80% POPE and 20% POPG, using the same buffer as above. The solution was tip-sonicated until a homogeneous distribution of vesicles with a mean radius of 100 nm was reached. The final concentration of P21 was 30 μM, and the lipid/peptide mole ratio was 100.

The samples of RSA, RNAse T_1, and azurin were prepared by dissolving the proteins in water to final concentrations of 20 μM (for RSA and RNAse) or 10 μM (for azurin). In the case of RSA, the aqueous solution contained 10 mM Na_2SO_4 and was buffered at pH 7.2 by 100 mM sodium phosphate, in the case of RNAse T_1 it contained no salt and was buffered at pH 5.5 by 100 mM sodium acetate, and in the case of azurin it contained 150 mM NaCl and was buffered at pH 7.4 by 50 mM sodium phosphate.

The samples of NATA were prepared from stock solutions of NATA in methanol (100 mM) and dilution to a final concentration of 50 μM in the different solvents. The aqueous solution was buffered at pH 7.0 by 1 mM Tris.

For each sample, a background control was prepared in exactly the same way by omitting the fluorescent substance.

Fluorescence measurements

The apparatus used has been described previously (Best et al. 1987; John and Jähnig 1988). As light source a modelocked YAG-laser and a cavity-dumped dye laser (Spectra Physics) with rhodamine 6G as dye was used. The final pulse repetition rate was 4.1 MHz. The wavelength of the excitation light was 300 nm and its intensity could be varied by means of two polarizers of which the first is rotatable and the second is fixed such that the polarization

of the excitation light is perpendicular to the scattering plane. The fluorescence light was observed at right angles to the excitation light. It passed through a prism polarizer to select polarizations parallel and perpendicular to the initial polarization providing the intensities $i_{\parallel}(t)$ and $i_{\perp}(t)$. Thereafter, it passed through a long-pass filter (Schott, model WG345/4) and a monochromator (Kratos, model 1500) set at 360 nm, and was detected by a photomultiplier tube (Philips, model XP2020Q) followed by single-photon counting electronics (EG & G). To avoid pulse pile-up, the count rate was kept below 1% of the pulse repetition rate (O'Connor and Phillips 1984) and routinely was at $4 \cdot 10^4$ counts/s. This was achieved by adjusting the intensity of the excitation light individually for each sample by rotating the first polarizer in the path of the excitation light. In the multichannel analyzer, data were collected until typically 10^7 counts in the channel of maximal intensity were reached. The time window was usually set at about 65 ns by choosing a time-to-channel ratio of 131.6 ps/ch for 512 channels. A typical measurement took about 12 h, requiring a high stability of the laser system. The temperature was kept constant at 22 °C.

The long sampling time gave rise to a new complication. Owing to the high number of counts in the first half of the channels, the signal-to-noise ratio there increased and oscillations appeared. They have been described previously and originate from crosstalk in the discriminator circuits and methods to eliminate them have been proposed (Holtom 1990; Small 1991). Unfortunately, these methods did not work in our hands so that we had to develop another strategy. We measured roomlight in the time-resolved mode, i.e. the laser pulse provided the start signal and roomlight the stop signal (or vice versa). Since there is no correlation between these two signals, a constant number of counts in time is expected. If, however, the discriminator circuits give rise to oscillations, they are detected at high enough numbers of counts. In this way, a correction factor for each channel could be derived and the measured curves be corrected.

The background controls for the samples were measured and corrected in the same way and their intensities $i^b_{\parallel}(t)$ and $i^b_{\perp}(t)$ subtracted from those of the samples $i^s_{\parallel}(t)$ and $i^s_{\perp}(t)$ yielding the polarized fluorescence intensities as $i_{\parallel}(t) = i^s_{\parallel}(t) - i^b_{\parallel}(t)$ and $i_{\perp}(t) = i^s_{\perp}(t) - i^b_{\perp}(t)$. The time courses of these intensities reflect (i) the time course of the exciting laser light, (ii) the decay of the polarized fluorescence intensities, and (iii) the characteristics of the detection system. To extract the decay of the polarized fluorescence intensities (ii), the effects of (i) and (iii) have to be eliminated by deconvolution of $i_{\parallel}(t)$ and $i_{\perp}(t)$ with the apparatus response function. Since the experimental determination of the response function poses problems, it was avoided by employing a fluorescence standard with a strict mono-exponential decay (Wahl et al. 1974; Libertini and Small 1984). We used PTP in cyclohexane with a lifetime of $\tau_S = 0.99$ ns (Wijnaendts van Resandt et al. 1982).

The time courses of the deconvoluted polarized fluorescence intensities again represent a superposition of two effects: (a) the decay of the total fluorescence intensity, and (b) the orientational motion of the fluorophore. In principle, the decay of the total fluorescence intensity can be obtained from a single measurement with the polarizer set at the magic angle of 54.7 °. However, our measurements were performed routinely at the two angles of 0 ° for parallel polarization and 90 ° for perpendicular polarization. In this case, the total fluorescence intensity is obtained as $s(t) = i_{\parallel}(t) + 2\beta i_{\perp}(t)$, with β denoting a correction factor for the polarization dependence of the monochromator, and the anisotropy is obtained as $r(t) = i_{\parallel}(t) - \beta i_{\perp}(t)\ s(t)$. The correction factor $\beta = 1.06$ was determined by performing measurements on the fluorophore phenanthrene with a lifetime of about 15 ns in cyclohexane and requiring that its anisotropy at long times vanishes.

The data were analyzed by assuming a multi-exponential decay for the total fluorescence intensity, $S(t) = \Sigma\, a_i \exp(-t/\tau_i)$, and for the anisotropy a multi-exponential decay with a residual anisotropy at long times, $R(t) = \Sigma\, b_i \exp(-t/\phi_i) + R_\infty$. The components of the polarized fluorescence then follow as $I_{\parallel}(t) = [S(t) + 2R(t)]/3$ and $I_{\perp}(t) = [S(t) - R(t)]/3\beta$. These quantities were convoluted with the apparatus response function (more exactly its replacement by the fluorescence standard), and a nonlinear least-square fit to the experimental data for $i_{\parallel}(t)$ and $i_{\perp}(t)$ was performed by varying a_i, τ_i, b_i, ϕ_i, and R_∞. Visual inspection of the residuals and a χ^2-test were taken as criteria for the best fit. We always started with a mono-exponential curve for the total fluorescence and then included stepwise more lifetimes until no further lifetime was resolved, i.e. one lifetime appeared twice.

Some remarks on the presentation of the data are necessary. (i) Only the decay of the total fluorescence intensity given by the sum s(t) is plotted and discussed, the anisotropy is not considered. (ii) Presentation of s(t) implies that the background has already been subtracted. (iii) The curves for s(t) level off at long times. The residual fluorescence intensity at long times is caused by residual laser light which appears owing to incomplete suppression of the laser light at long times and which gives rise to new excitations of the fluorescence. Since the residual light is distributed homogeneously in time, the residual fluorescence is detected in the same way as the steady-state fluorescence and is proportional to it. (iv) The experimental data on s(t) for different samples presented in one figure were normalized to equal sampling times which under the condition of a constant count rate implies a constant total number of counts or constant area under the curves for s(t). This is equivalent to a constant steady-state intensity, hence, the data are presented under the condition of a constant steady-state intensity. In this case, the residual fluorescence at long times being proportional to the steady-state fluorescence is the same for different samples.

Control measurements and control evaluations

Control measurements for the total fluorescence intensity were carried out by performing measurements on LP in lipid with the polarizer set at the magic angle of 54.7 °. They led to the same result as the determination by measurements of $i_{\parallel}(t)$ and $i_{\perp}(t)$. This indicates that the value of the correction factor β has been determined correctly.

As a further control, measurements on LP in lipid were repeated using the same sample. If the existence of a long lifetime resulted from destruction of tryptophan by laser light and the appearance of a photo product, the effect would be additive in two consecutive measurements and the amplitude of the long lifetime component should increase by a factor of two in the second measurement. This was not observed and, therefore, we exclude the possibility that the long lifetime component arises from a photo product.

A series of control measurements and evaluations were carried out on NATA in water to investigate the dependence of the result for the fluorescence decay parameters on various parameters such as (i) the emission wavelength λ_{em}, (ii) the time window T, (iii) the time-to-channel ratio s, and (iv) the assumed lifetime τ_S of the fluorescence standard. The quantities λ_{em} and T are experimental parameters and control measurements at different λ_{em} and T had to be performed, while s and τ_S are parameters in the data analysis and require control evaluations using different values of s and τ_S. As demonstrated by the data in Table 1, a variation of the emission wavelength λ_{em} between 340 nm and 360 nm leaves the decay parameters essentially unaffected. The time-to-channel ratio s also leaves the mean lifetime $\langle\tau\rangle$ unchanged, but affects the weak second lifetime component. The lifetime τ_S of the fluorescence standard has a minor effect on $\langle\tau\rangle$, but a strong effect on the two lifetime components. Measured values of the lifetime of PTP are 0.95 ns (Berlman 1971), 0.97 ns (John and Jähnig 1988), and 0.99 ns (Wijnaendts van Resandt et al. 1982). Based on the data of Table 1, we consider the values $\tau_S = 0.99$ ns to be the most reliable one and will use it here.

The time window T is of special relevance for our purposes. Figure 1 shows the results for a time window of 20 ns. A mono-exponential fit of the data yields a lifetime of 2.97 ns. When a second lifetime is permitted in the fit, a long lifetime of 16 ns with a small amplitude of 0.1% is obtained. The determination of a lifetime of 16 ns within a time window of 20 ns and with an intensity of about 10^5 counts at the maximum, however, is not very reliable. Therefore, we repeated this measurement with a time window of 65 ns and an intensity of about 10^6 counts at the maximum. As shown in Fig. 2, the measured intensity decreases over about 40 ns and then levels off. This leveling off may be caused by (i) a background fluorescence, (ii) a long lifetime component, or (iii) new excitations of the fluorescence due to incomplete suppression of the laser light after the pulse. The background fluorescence has already been subtracted from the data, so that it can not be responsible for the leveling off. Assuming a mono-exponential decay a good fit is obtained with a lifetime of 2.96 ns. When a second lifetime is permitted in the fit, a single liefetime of 2.96 ns is still obtained. Hence, the fluorescence decay of NATA in water is mono-exponential and the leveling off is caused by new excitations of the fluorescence. The lifetime results as 2.96 ns and thus lies within the spread of the data from the literature (Table 1).

Table 1. Influence of the excitation wavelength λ_{ex}, the emission wavelength λ_{em}, the time/channel ratio s, the lifetime τ_S of the fluorescence standard, and the time window T on the lifetimes and amplitudes (in brackets) of NATA in water. For comparison, data from the literature are included

λ_{ex} (nm)	λ_{em} (nm)	s (ns)	τ_S (ps/ch)	T (ns)	τ_1 (ns)	τ_2 (ns)	$\langle\tau\rangle$ (ns)	χ^2
300	360	42.02[a]	0.99	20	2.94 (0.997)	9.87 (0.003)	2.96	1.47
300	340	42.02	0.99	20	2.93 (0.997)	9.80 (0.003)	2.95	1.97
300	360	41.84[a]	0.99	20	2.94 (0.999)	16.18 (0.001)	2.95	1.49
300	360	42.02	0.97	20	2.75 (0.83)	3.74 (0.17)	2.92	1.56
300	360	131.6	0.99	65	2.96 (1.000)	16.18[b] ($<5\times10^{-5}$)	2.96	1.47
295[c]	355	87		35	3.00		3.00	
295[d]	340	37	0.99	25	3.05		3.05	
295[e]	>320		scatt[h]	12.5	2.95		2.95	
280[f]	330	43	scatt	20	3.00		3.00	
280[g]	350	12		25	0.50 (0.03)	3.10 (0.97)	3.02	

[a] The difference between the two values of 42.02 and 41.84 ps/ch for the ratios corresponds to an uncertainty of one channel in the determination of s and, therefore, respresents an upper limit for the error in s

[b] The lifetimes τ_1 and τ_2 were kept constant and the amplitude of τ_2 was decreased until the calculated curve in Fig. 2a came to lie within the scattering of the data

[c] Data from Ross et al. (1981)

[d] Data from Wijnaendts van Resandt et al. (1982)

[e] Data from Petrich et al. (1983)

[f] Data from Szabo and Rayner (1980)

[g] Data from Vekshin et al. (1992)

[h] Scattering of light was used to determine the apparatus response function

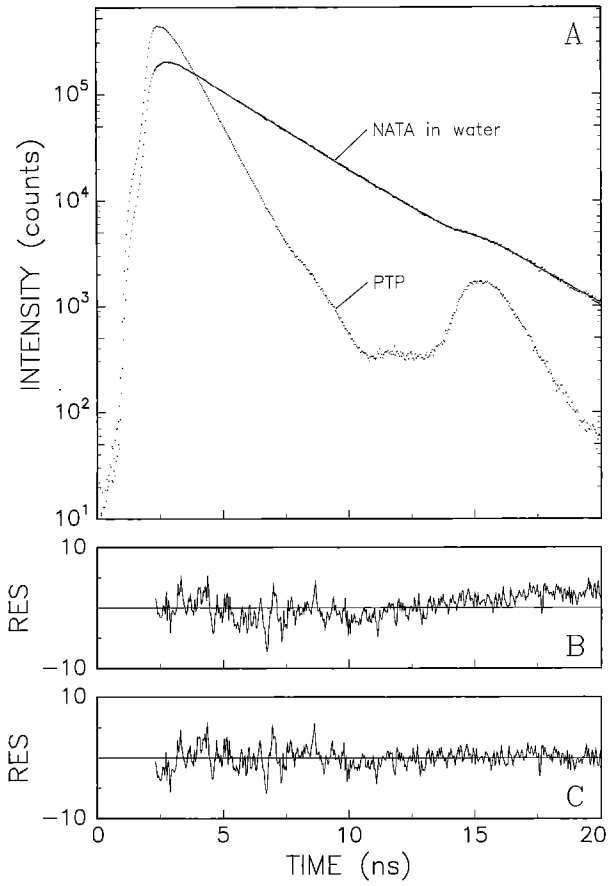

Fig. 1 A–C. Temporal decay in a time window of 20 ns of the fluorescence of NATA in water. **A** The experimental data are shown (*dots*) together with those for the fluorescence standard PTP (*dots*, *lower curve*), normalized to equal sampling times. Included are the best fits by a mono-exponential (——) and a double-exponential (- - -) curve after convolution with the apparatus response function. **B**, **C** The residuals of the best fits by a *mono-exponential* **B** and a double-exponential **C** curve are also shown

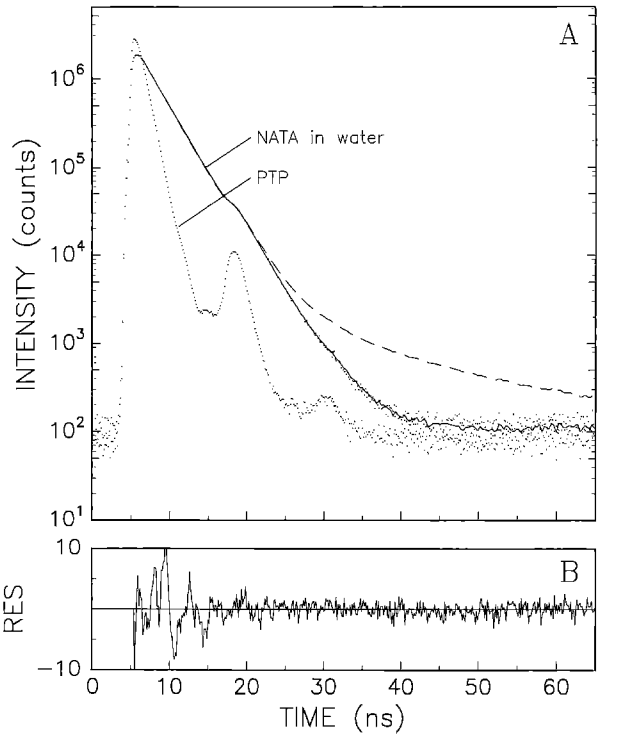

Fig. 2 A, B. Temporal decay in a time window of 65 ns of the fluorescence of NATA in water. **A** The experimental data are shown (*dots*) together with those for the fluorescence standard PTP (*dots*, *lower curve*), normalized to equal sampling times. Included are the best fit by a mono-exponential curve (——) and a double-exponential curve (- - -) with τ_1 as obtained from the mono-exponential fit and $\tau_2 = 16.18$ ns with an amplitude of 0.001, both after convolution with the apparatus response function. **B** The residuals of the best fit by a mono-exponential curve are also shown

If the previous second lifetime of 16 ns with an amplitude of 0.1% is included in the calculated decay curve, the curve at long times deviates strongly from the experimental data, as shown in Fig. 2. To come within the scatter of the experimental data, the amplitude of the long lifetime component would have to be smaller than $5 \cdot 10^{-5}$. If the second lifetime is assumed to be 25 ns, as will be found for several proteins, the amplitude would have to be below 10^{-5} to be compatible with the experimental data of Fig. 2. Hence, the fluorescence of NATA in water is mono-exponential within the limit of 10^{-5} for the amplitude of a 25 ns lifetime component.

The χ^2 values obtained by us for the measurements on NATA are comparable to those found in the literature (Table 1). For the measurements on proteins with a long lifetime component of the Trp fluorescence and therefore higher numbers of counts at the maximum, the χ^2 values were larger. The reason for that lies in the oscillations of the measured intensities due to crosstalk in the discriminator circuits as discussed above and non-perfect correction for them.

The data might have been fitted by distributions of lifetimes (Alcala et al. 1987a). This would have led to some spreading of the individual lifetime components, but not to qualitatively different results.

Results

Outer membrane protein A

OmpA is a protein of the outer membrane of *Escherichia coli*. Its membrane-incorporated part contains a high degree of β-structure and presumably forms a β-barrel (Vogel and Jähnig 1986). OmpA has 5 Trp residues which according to structure predictions are all located on membrane-spanning β-strands. It was investigated because it can easily be unfolded in GdHCl and refolded into lipid membranes (Surrey and Jähnig 1992). Measurements were performed on OmpA either dissolved and unfolded in GdHCl or reconstituted in lipid vesicles of 80% POPC and 20% POPG.

The results of the time-resolved measurements of the Trp fluorescence of OmpA in the unfolded and folded form are shown in Fig. 3. The experimental data are presented together with the fits by multi-exponential curves after

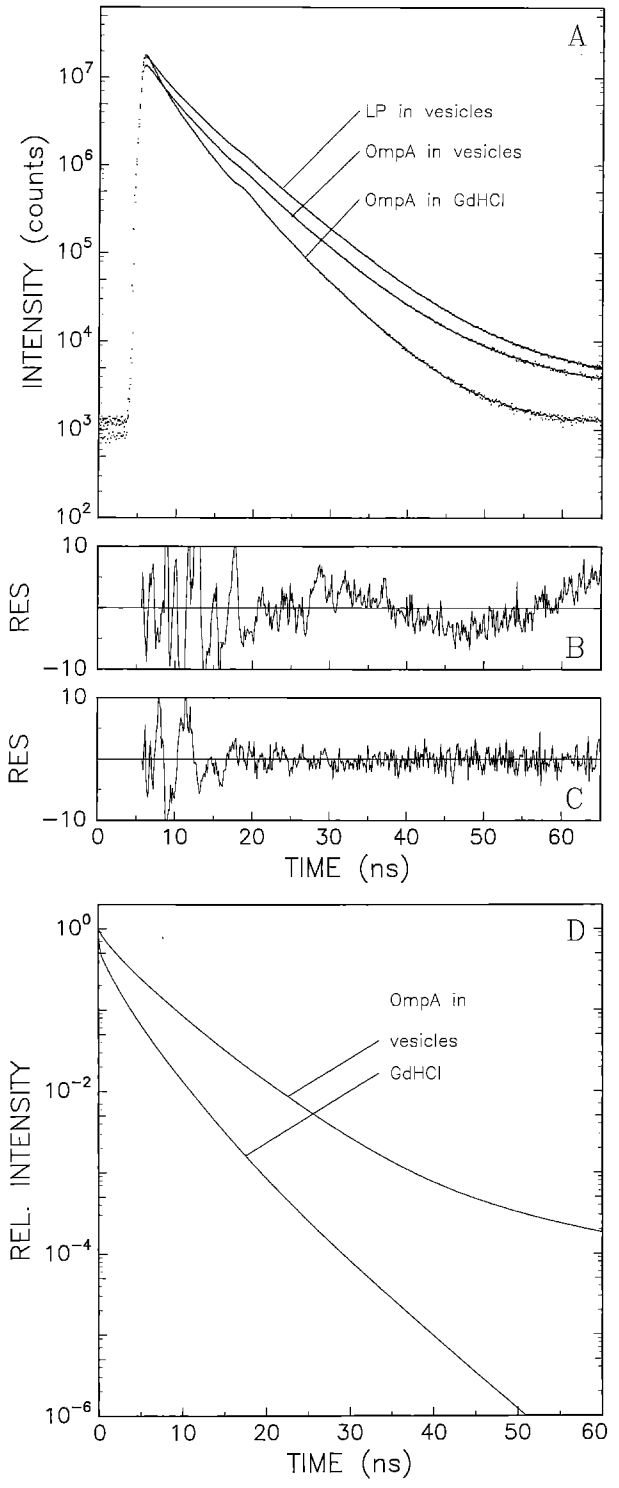

Fig. 3 A–D. Temporal decay of the tryptophan fluorescence of OmpA dissolved and unfolded in 6 M GdHCl, OmpA reconstituted in lipid vesicles of 80% POPC and 20% POPG, and LP reconstituted in lipid vesicles of 80% POPE and 20% POPG. **A** The experimental data (*dots*) for the three cases are shown, all normalized to equal sampling times. Included are the best fits by multi-exponential curves after convolution with the apparatus response function (*lines*). **B, C** Residuals of the two fits with 4 **B** and 5 **C** lifetime components for the case of OmpA reconstituted in lipid vesicles. They lead to χ^2 values of 11.71 **B** and 7.02 **C**. **D** Multi-exponential decay curves of the fluorescence for the two cases of OmpA unfolded in GdHCl and reconstituted in lipid vesicles as determined by the fits, without convolution with the apparatus response function

convolution with the apparatus response function. The decay is more rapid for the unfolded than for the folded form. In both cases, the intensity starts from a maximum of about 10^7 counts, decreases rather monotonically over an extended period of time, and then levels off. This leveling off may be caused by new excitations of the fluorescence due to incomplete suppression of the laser light after the pulse or by a long lifetime component of the fluorescence decay. A careful analysis of the data shows that for unfolded OmpA the leveling off is caused by new excitations of the fluorescence, while for folded OmpA a long lifetime component is responsible.

The numerical results of the analysis in terms of multi-exponential decays are listed in Table 2. For unfolded OmpA, the best fits were obtained with 4 exponentials, the values of the 4 lifetimes being typical for proteins. It has been shown that unfolded proteins exhibit rather uniform fluorescence decay characteristics with two lifetimes of about 1.3 and 3.7 ns (Grinvald and Steinberg 1976). Our result for unfolded OmpA fits into this scheme, if the shortest and longest lifetimes are neglected. They may not have been resolved in the earlier studies. For folded OmpA, a fit with 4 exponentials leads to residuals with smooth oscillations at longer times (Fig. 3 B) and a value of $\chi^2 = 11.71$. Such oscillations are indicative of a hidden exponential, and a fit with 5 exponentials indeed improves the residuals (Fig. 3 C) and the χ^2 value decreases to 7.02. The fifth lifetime has a value of 25 ns with an amplitude of 0.2%. The error in both quantities is about 10%. The multi-exponential decay curves of the tryptophan fluorescence of folded and unfolded OmpA are compared in Fig. 3 D. Although of small amplitude, the long lifetime component dominates the fluorescence of folded OmpA in lipids at long times.

Lactose permease

LP is also a membrane protein of *Escherichia coli* and was investigated only in the folded form, reconstituted in lipid vesicles of 80% POPE and 20% POPG. According to the best structural data available, LP is folded in 12 membrane-spanning helices and the 6 Trp residues are all located on membrane-spanning helices (Kaback et al. 1990).

The experimental data for reconstituted LP are included in Fig. 3 A. The intensity behaves in a similar way as for folded OmpA, it first decreases monotonically and then levels off. The analysis of the data shows that the leveling off is again caused by a long lifetime component.

The numerical result of the analysis in terms of multi-exponential decays is included in Table 2. Again the best fit was obtained for 5 exponentials. The long lifetime has a value of 30 ns with an amplitude of 0.1%.

Peptide P 21

P 21 is a hydrophobic peptide and is therefore insoluble in water. In an apolar environment, it forms an α-helix with the single Trp residue close to the C-terminal end. When incorporated in lipid membranes, the helix spans the bi-

Table 2. Fluorescence lifetimes τ_i and relative amplitudes a_i (in brackets) of different proteins and NATA in different environments

Sample	τ_1 (ns)	τ_2 (ns)	τ_3 (ns)	τ_4 (ns)	τ_5 (ns)	$\langle\tau\rangle$ (ns)	χ^2
OmpA in							
GdHCl	0.1	1.5	3.0	5.0		1.3	7.53
	(0.47)	(0.25)	(0.25)	(0.03)			
lipid	0.4	1.7	3.6	6.0	25.4	3.9	7.02
	(0.08)	(0.15)	(0.45)	(0.32)	(0.002)		
LP in							
lipid	0.6	2.6	5.0	7.0	30.3	4.0	6.82
	(0.17)	(0.23)	(0.44)	(0.16)	(0.001)		
P21 in							
lipid	0.5	1.5	3.1	5.4	26.7	1.9	4.11
	(0.32)	(0.33)	(0.25)	(0.09)	(0.001)		
butanol	0.2	1.7	4.4	6.3	23.6	4.7	2.26
	(0.01)	(0.20)	(0.33)	(0.45)	(0.002)		
NATA in							
water			3.0			3.0	1.47
butanol			3.5			3.5	2.46
GdHCl			2.8			2.8	2.23
GdHCl[a]	0.01		2.98			2.95	
	(0.01)		(0.99)				
RSA in							
water	0.2	2.7	6.5	9.5		5.1	8.35
	(0.22)	(0.14)	(0.46)	(0.18)			
water[b]	0.3	2.2	5.8	9.8		3.8	
	(0.33)	(0.16)	(0.39)	(0.11)			
RNAse T_1 in							
water		1.7	3.9	4.9		3.8	5.48
		(0.08)	(0.88)	(0.04)			
water[c]		1.8	3.7			3.4	1.49
		(0.17)	(0.83)				
Azurin in							
water	0.5	1.2	3.5	6.5	23.0	1.3	7.92
	(0.60)	(0.22)	(0.14)	(0.05)	(0.001)		
water[d]	0.2		4.8			1.2	
	(0.79)		(0.21)				

[a] Data from Bismuto et al. (1991) for NATA in 6 M GdHCl, 0.1 M sodium phosphate, pH 7
[b] Data from Gentin et al. (1990) for RSA in buffer, $\lambda_{ex} = 300$ nm, $\lambda_{em} > 360$ nm
[c] Data from MacKerell et al. (1987) for RNAse T_1 in buffer at 40 °C, $\lambda_{ex} = 300$ nm, $\lambda_{em} = 380$ nm
[d] Data from Szabo et al. (1983) for azurin in buffer at pH 5.3, $\lambda_{ex} = 290$ nm, $\lambda_{em} = 345$ nm

layer (Voges et al. 1987; Vogel et al. 1988). P21 was investigated in the folded form, either dissolved in butanol or incorporated in lipid vesicles.

The experimental data for P21 in butanol and in lipid vesicles are shown in Fig. 4. The decay is faster for P21 incorporated in lipid vesicles than dissolved in butanol. The analysis of the data shows that in both cases the leveling off is caused by a long lifetime component.

The numerical results of the analysis are included in Table 2. In both cases, the data are fitted best by 5 exponentials. The 4 short lifetimes and the long lifetime of 25 ns are comparable to those of OmpA and LP in lipid vesicles. The amplitude of the long lifetime is also in the same range of 0.1%–0.2%.

NATA

NATA is soluble in solvents of different polarity and was investigated in water, butanol, and GdHCl. The experimental data for NATA in water were presented and discussed under Materials and Methods, the data for NATA in butanol are included in Fig. 4. In all cases, the intensity decay is mono-exponential, a long lifetime component is absent. This is rather obvious from a comparison of the curves for NATA and P21 in butanol (Fig. 4).

The numerical results of the data analysis are included in Table 2. The fluorescence of NATA has a lifetime of 3.0 ns in water, 3.5 ns in butanol, and 2.8 ns in GdHCl. For the latter case, roughly the same result was found by Bismuto et al. (1991).

Rat serum albumin

RSA is a soluble protein and contains a single Trp residue, but its structure is not available. RSA was included in our studies as a control, since time-resolved fluorescence measurements on RSA have been reported recently by Gentin et al. (1990). The fluorescence decay shown in

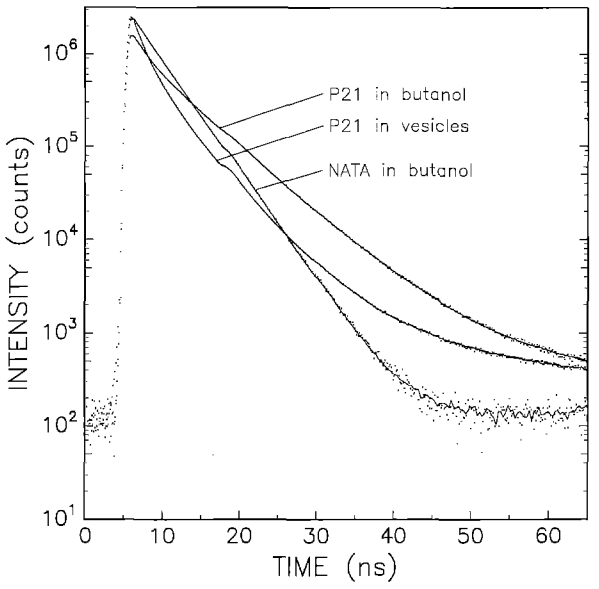

Fig. 4. Temporal decay of the tryptophan fluorescence of peptide P21 incorporated in lipid vesicles of 80% POPE and 20% POPG, and dissolved in butanol. For comparison, the data of NATA in butanol are included. The experimental data normalized to equal sampling times are shown (*dots*), together with the fits by multi-exponential curves after convolution with the apparatus response function (*lines*)

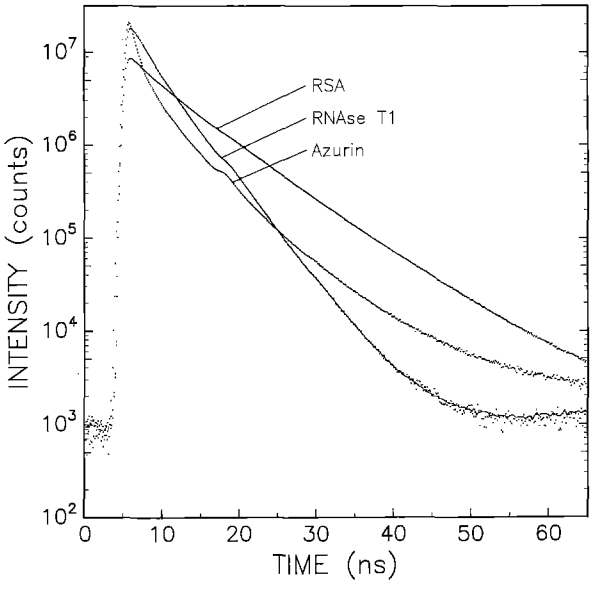

Fig. 5. Temporal decay of the tryptophan fluorescence of RSA, RNAse T_1, and azurin in water. The experimental data normalized to equal sampling times are shown (*dots*), together with the fits by multi-exponential curves after convolution with the apparatus response function (*lines*)

Fig. 5 is roughly mono-exponential, even at long times, because the level of the fluorescence due to new excitations at long times (as seen for RNAse T_1 in Fig. 5) has not yet been reached. Hence, a long lifetime component is absent in this case.

The numerical result of the data analysis is included in Table 2. Four lifetimes are sufficient to fit the data, the longest being 9.5 ns. The values for the lifetimes and their amplitudes are in rough agreement with the results of Gentin et al. (1990), the deviations summing up to about 25% in the mean lifetime (Table 2).

Ribonuclease T_1

RNAse T_1 is again a soluble protein with one Trp residue, but its structure is known from X-ray diffraction (Heinemann and Saenger 1982). The Trp residue is located in the cleft forming the nucleotide binding site. The fluorescence decay of RNAse T_1 is included in Fig. 5 and shows a rather mono-exponential behaviour, the leveling off at long times being caused by new excitations of the fluorescence. Hence, a long lifetime component is absent also in this case.

The numerical results of the data analysis are included in Table 2. Three lifetime components are sufficient to fit the data, the two fast ones of 1.7 ns and 3.9 ns providing 96% of the intensity. This result is in good agreement with the finding of MacKerell et al. (1987) (Table 2).

Azurin

Azurin is again a soluble protein with one Trp residue whose structure has been determined by X-ray diffraction (Adman et al. 1978). The Trp residue is located in the center of a β-barrel. The fluorescence decay is included in Fig. 5 and does not exhibit mono-exponential behaviour. The detailed analysis of the data reveals that the leveling off at long times is no longer caused by new excitations of the fluorescence, but by a long lifetime component.

The numerical results of the data analysis are included in Table 2. Five lifetime components are required to fit the data, the long lifetime being 23 ns. The shorter lifetimes are in rough agreement with the earlier finding of Szabo et al. (1983) (Table 2).

Discussion

In 5 of the 11 cases investigated, the tryptophan fluorescence exhibited a long lifetime component between 23 ns and 30 ns. These 5 cases are OmpA and LP in lipid vesicles, peptide P21 in lipid vesicles and in butanol, and azurin in water. The 6 other cases, where no long lifetime component was found, are OmpA unfolded in GdHCl, NATA in 3 different solvents including butanol, as well as RSA and RNAse T_1 in water. These findings raise the obvious question: Is there a rule behind the occurrence of the long lifetime component and if so, what does this rule tell us about protein substates?

We first try to draw some conclusions from a comparison of the results for the two membrane proteins, the peptide, and NATA. The long lifetime occurred for OmpA and LP in lipid membranes as well as for the peptide in lipid membranes or butanol, but not for OmpA dissolved in GdHCl. Hence, as a first guess one might think of a hydrophobic environment around the tryptophan residues be-

ing necessary for the long lifetime component. Then, however, the long lifetime should also be found for NATA in butanol. This was not the case and, therefore, hydrophobicity is a necessary but not a sufficient condition for the long lifetime component to occur.

Attempting to deduce a further condition for the occurrence of the long lifetime, one may compare the peptide in butanol with NATA in butanol. For the peptide, the long lifetime occurred, for NATA not. The solvent was the same in both cases, but in the case of the peptide the tryptophan residue is part of a large molecule, while in the case of NATA it is isolated. Hence, one may conclude that attachment to a large molecule is necessary for the long lifetime. The case of OmpA in GdHCl, where the long lifetime did not occur, does not contradict this rule, because in this case the environment is not hydrophobic, and hydrophobicity was already recognized as a necessary condition. So we come to the conclusion that a hydrophobic environment and incorporation in a polypeptide chain are necessary for the long lifetime to occur.

This conclusion can be made more precise, when taking into account the rules which have been established for the structure of polypeptide chains in a hydrophobic environment, especially for membrane proteins (Kyte and Doolittle 1982; Eisenberg et al. 1986; Jähnig 1990). In a hydrophobic environment such as a lipid membrane, polypeptide chains must fold into an ordered structure, either an α-helix or a β-barrel, in order to saturate the hydrogen bonds of the backbone atoms. All available experimental data are consistent with this postulate. The above conditions for a long lifetime to occur may then be expressed in the following more precise manner: A long lifetime occurs when the tryptophan residue is in a hydrophobic environment and participates in an α-helix or a β-strand. Our results are consistent with this rule, since in the case of peptide P21 and LP the tryptophan residues participate in α-helices and in the case of folded OmpA they participate in β-strands. Previously, a long lifetime component has been observed for a synthetic analogue of melittin, but not for melittin (John and Jähnig 1988, 1992), and this difference may be explained along the same lines.

How do the results for soluble proteins fit into this rule? For RSA, structural data are not available, but for RNAse T_1 and azurin the structures are known (Heinemann and Saenger 1982; Adman et al. 1978). They reveal that the single tryptophan residues in both cases are located inside the proteins and participate in β-strands. Assuming that the interior of soluble proteins is hydrophobic, one would predict that a long lifetime component exists in both cases. However, while azurin exhibits a long lifetime, RNAse T_1 does not. Obviously, the question is how hydrophobic is the interior of soluble proteins. An indicator for that may be provided by the emission wavelength λ_{em} of the tryptophan fluorescence. For azurin, $\lambda_{em} = 308$ nm indicates a very hydrophobic environment of the tryptophan residue, while $\lambda_{em} = 325$ for RNAse T_1 nm is indicative of a weaker local hydrophobicity. The conclusion would be that for a long lifetime to occur a sufficiently strong hydrophobicity around the tryptophan residue is required. Actually, hydrophobicity may be considered in this case as a measure for the inaccessibility of the tryptophan residue to oxygen acting as a quencher. The tryptophan residue in azurin would then be less accessible to oxygen than in RNAse T_1, and the condition of a sufficiently hydrophobic environment for the long lifetime to occur would actually mean that the tryptophan residue is sufficiently inaccessible to oxygen. Further studies are required to put this hypothesis on a firm basis.

The requirement of an ordered structure for the long lifetime to occur may have some bearing on protein substates. As discussed in the Introduction, the occurrence of a long fluorescence lifetime requires the existence of substates with lifetimes at least as long. Our finding of a long lifetime of 25 ns for tryptophan residues participating in α-helices and β-barrels would thus indicate that α-helices or β-barrels have substates with lifetimes longer than 25 ns, while disordered structures would not have such long-lived substates. This seems conceivable since a conformational change of an ordered structure involves displacements of many atoms and, therefore, occurs rarely so that the protein remains in a given substate for a relatively long time. Within this scheme, the population of the long-lived substates of α-helices and β-barrels would be proportional to the amplitude of the long lifetime component and, thus, be very low.

The lifetimes of substates may be investigated directly by time-resolved fluorescence anisotropy measurements. The long lifetime component of the Trp fluorescence opens the way to extend such measurements to longer times than has been possible hitherto. Anisotropy measurements have always been hampered by the short lifetime of the Trp fluorescence. The amplitude of the long lifetime component is very small, 0.1–0.2%, and at first sight may seem negligible. The point is that at sufficiently long times the long lifetime component becomes the dominant component in the fluorescence intensity. At about 40 ns, the intensity of the long lifetime component already equals the intensity of the sum of the short component, and at 65 ns it is an order of magnitude larger. Therefore, the long lifetime may be useful for measurements over such long times. In the past, such measurements have been performed using extrinsic labels with long lifetimes (Dornmair and Jähnig 1989). With such labels, however, there is always the danger that they do not accurately reflect the dynamics of the unlabeled protein, and measurements using intrinsic Trp fluorescence are therefore preferable.

Acknowledgements. We thank P. Nollert from our institute and E. John from Ciba-Geigy in Basel for their help and advice, W. Beck and G. Jung from the University of Tübingen for the gift of peptide P21, S. Walter and F.X. Schmid from the University of Bayreuth for the gift of ribonuclease T_1, and R. Eser from Spectra Physics for expert support with the laser system.

References

Adman ET, Stenkamp RE, Sieker LC, Jensen LH (1978) A crystallographic model for azurin at 3 Å resolution. J Mol Biol 123:35–47

Alcala JR, Gratton E, Prendergast Fg (1987a) Interpretation of fluorescence decays in proteins using continuous lifetime distributions. Biophys J 51:925–936

Alcala JR, Gratton E, Prendergast FG (1987b) Fluorescence lifetime distributions in proteins. Biophys J 51:597–604

Ansari A, Berendzen J, Bowne SF, Frauenfelder H, Iben IET, Sauke TB, Shyamsunder E, Young RD (1985) Protein states and proteinquakes. Proc Natl Acad Sci, USA 82:5000–5004

Bajzer Z, Prendergast FG (1993) A model for multi-exponential tryptophan fluorescence intensity decay in proteins. Biophys J 65:2313–2323

Beecham JM, Brand L (1985) Time-resolved fluorescence of proteins. Anu Rev Biochem 54:43–71

Berlman I (1971) Handbook of fluorescence spectra of aromatic molecules. Academic Press, New York

Best L, John E, Jähnig F (1987) Order and fluidity of lipid membranes as determined by fluorescence anisotropy decay. Eur Biophys J 15:87–102

Bismuto E, Sirangelo I, Irace G (1991) Conformational dynamics of unfolded peptides as a function of chain length: A frequency domain fluorescence approach. Arch Biochem Biophys 291:38–42

Chang MC, Petrich JW, McDonald DB, Fleming GR (1983) Non-exponential fluorescence decay of tryptophan, tryptophylglycine, and glycyltryptophan. J Am Chem Soc 105:3819–3824

Dornmair K, Jähnig F (1989) Internal dynamics of lactose permease. Proc Natl Acad Sci, USA 86:9827–9831

Eisenberg DM, Steitz TA, Goldman A (1986) Identifying nonpolar transbilayer helices in amino acid sequences of membrane proteins. Anu Rev Biophys Chem 15:321–353

Gallay J, Vincent M, de la Sierra IML, Alvarez J, Ubieta R, Madrazo J, Padron G (1993) Protein flexibility and aggregation state of human epidermal growth factor. Eur J Biochem 211:213–219

Gentin M, Vincent M, Brochon JC, Livesey AK, Cittanova N, Gallay J (1990) Time-resolved fluorescence of the single tryptophan residue in rat α-fetoprotein and rat serum albumin: Analysis by the maximum-entropy method. Biochemistry 29:10405–10412

Godik VI, Blankenship RE, Causgrove TP, Woodbury N (1993) Time-resolved tryptophan fluorescence in photosynthetic reaction centers from Rhodobacter sphaeroides. FEBS Lett 321: 229–232

Grinvald A, Steinberg IZ (1976) The fluorescence decay of tryptophan residues in native and denatured proteins. Biochim Biophys Acta 427:663–678

Heinemann U, Saenger W (1982) Specific protein-nucleic acid recognition in ribonuclease T_1-2′-guanylic acid complex: an X-ray study. Nature 299:27–31

Holtom GR (1990) Artifacts and diagnostics in fast fluorescence measurements. In: Lakowicz JR (ed) Time-resolved laser spectroscopy in biochemistry III, SPIE proceedings, vol 1204, SPIE, Bellingham, WA, pp 2–12

Jähnig F (1990) Structure predictions of membrane proteins are not that bad. Trends Biochem Sci 15:93–95

John E, Jähnig F (1988) Dynamics of melittin in water and membranes as determined by fluorescence anisotropy decay. Biophys J 54:817–827

John E, Jähnig F (1992) A synthetic analogue of melittin aggregates in large oligmers. Biophys J 63:1563–1543

Kaback HR, Bibi E, Roepe PD (1990) β-Galactoside transport in E. coli: A functional dissection of lac permease. TIBS 15:309–314

Kyte J, Doolittle RF (1982) A simple method for displaying the hydropathy character of a protein. J Mol Biol 157:105–132

Libertini LJ, Small EW (1984) F/F deconvolution of fluorescence decay data. Anal Biochem 138:314–318

MacKerell AD, Rigler R, Nilsson L, Hahn U, Saenger W (1987) A time-resolved fluorescence, energetic and molecular dynamics study of ribonuclease T_1. Biophys Chem 26:247–261

O'Connor DV, Phillips D (1984) Time-correlated single photon counting. Academic Press, London

Petrich JW, Chang Mc, McDonalds DB, Fleming GR (1983) On the origin of non-exponential fluorescence decay in tryptophan and its derivatives. J Am Chem Soc 105:3824–3832

Robbins RJ, Fleming GR, Beddard GS, Robinson GW, Thistlethwaite PF, Woolfe GJ (1980) Photophysics of aqueous tryptophan: pH and temperature effects. J Am Chem Soc 102: 6271–6279

Ross JBA, Rousslang KW, Brand L (1981) Time-resolved fluorescence and anisotropy decay of the tryptophan in adrenocorticotropin = (1–24). Biochemistry 20:4361–4369

Small EW (1991) Laser sources and microchannel plate detectors for pulse fluorometry. In: Lakowicz JR (ed) Topics in fluorescence spectroscopy, vol 1. Plenum, New York, pp 97–182

Surrey T, Jähnig F (1992) Refolding and oriented insertion of a membrane protein into a lipid bilayer. Proc Natl Acad Sci, USA 89:7457–7461

Szabo AG, Rayner DM (1980) Fluorescence decay of tryptophan conformers in aqueous solution. J Am Chem Soc 102:554–563

Szabo AG, Stepanik TM, Wayner DM, Young NM (1983) Conformational heterogeneity of the copper binding site in azurin. Biophys J 41:233–244

Vekshin N, Vincent M, Gallay J (1992) Excited-state lifetime distributions of tryptophan fluorescence in polar solvents. Evidence for solvent exciplex formation. Chem Phys Lett 199:459–464

Vogel H, Jähnig F (1986) The structure of melittin in membranes. Biophys J 50:573–582

Vogel H, Nilsson L, Rigler R, Voges KP, Jung G (1988) Structural flucutations of a helical polypeptide traversing a lipid bilayer. Proc Natl Acad Sci, USA 85:5067–5071

Voges KP, Jung G, Sawyer WH (1987) Depth-dependent fluorescent quenching of a tryptophan residue located at defined positions on a rigid 21-peptide helix in liposomes. Biochim Biophys Acta 896:64–76

Wagner BD, James DR, Ware WR (1987) Fluorescence lifetime distributions in homotryptophan derivatives. FEBS Lett 138: 181–184

Wahl P, Auchet JC, Donzel B (1974) The wavelength dependence of the response of a pulse fluorimeter using the single photoelectron counting method. Rev Sci Instrum 45:28–32

Wijnaendts van Resandt RW, Vogel RH, Provencher SW (1982) Double beam fluorescence lifetime spectrometer with subnanosecond resolution: Application to aqueous tryptophan. Rev Sci Instrum 53:1392–1397